

# Muscle MRI in periodic paralysis shows myopathy is common and correlates with intramuscular fat accumulation

Vinojini Vivekanandam MBBS<sup>1</sup>  | Karen Seutterlin PhD<sup>1,2</sup> |  
 Emma Matthews PhD<sup>3</sup> | John Thornton PhD<sup>4</sup> | Dipa Jayaseelan PhD<sup>1</sup> |  
 Sachit Shah PhD<sup>4</sup> | Jasper M. Morrow PhD<sup>1</sup> | Tarek Yousry PhD<sup>4</sup> |  
 Michael G. Hanna FMedSci<sup>1</sup>

<sup>1</sup>Queen Square Centre for Neuromuscular Diseases, UCL Queen Square Institute of Neurology, London, UK

<sup>2</sup>AGE Research Group, NIHR Newcastle Biomedical Research Centre, Newcastle upon Tyne Hospitals NHS Foundation Trust and Newcastle University, Newcastle upon Tyne, UK

<sup>3</sup>Atkinson-Morley Neuromuscular Centre, Department of Neurology, St George's University Hospitals NHS Foundation Trust, and Molecular and Clinical Sciences Research Institute, St George's University of London, London, UK

<sup>4</sup>Neuroradiological Academic Unit, UCL Queen Square Institute of Neurology, UCL, London, UK

## Correspondence

Vinojini Vivekanandam, Queen Square Centre for Neuromuscular Diseases, UCL Queen Square Institute of Neurology, London, UK.  
 Email: [v.vivekanandam@ucl.ac.uk](mailto:v.vivekanandam@ucl.ac.uk)

Sachit Shah, Neuroradiological Academic Unit, UCL Queen Square Institute of Neurology, UCL, London, UK.  
 Email: [sachit.shah@nhs.net](mailto:sachit.shah@nhs.net)

## Abstract

**Introduction/Aims:** The periodic paralyses are muscle channelopathies: hypokalemic periodic paralysis (*CACNA1S* and *SCN4A* variants), hyperkalemic periodic paralysis (*SCN4A* variants), and Andersen-Tawil syndrome (*KCNJ2*). Both episodic weakness and disabling fixed weakness can occur. Little literature exists on magnetic resonance imaging (MRI) in muscle channelopathies. We undertake muscle MRI across all subsets of periodic paralysis and correlate with clinical features.

**Methods:** A total of 45 participants and eight healthy controls were enrolled and underwent T1-weighted and short-tau-inversion-recovery (STIR) MRI imaging of leg muscles. Muscles were scored using the modified Mercuri Scale.

**Results:** A total of 17 patients had *CACNA1S* variants, 16 *SCN4A*, and 12 *KCNJ2*. Thirty-one (69%) had weakness, and 9 (20%) required a gait-aid/wheelchair. A total of 78% of patients had intramuscular fat accumulation on MRI. Patients with *SCN4A* variants were most severely affected. In *SCN4A*, the anterior thigh and posterior calf were more affected, in contrast to the posterior thigh and posterior calf in *KCNJ2*. We identified a pattern of peri-tendinous STIR hyperintensity in nine patients. There were moderate correlations between Mercuri, STIR scores, and age. Intramuscular fat accumulation was seen in seven patients with no fixed weakness.

**Discussion:** We demonstrate a significant burden of disease in patients with periodic paralyses. MRI intramuscular fat accumulation may be helpful in detecting early muscle involvement, particularly in those without fixed weakness. Longitudinal studies are needed to assess the role of muscle MRI in quantifying disease progression over time and as a potential biomarker in clinical trials.

**Abbreviations:** ATS, Andersen-Tawil syndrome; EDL, extensor digitorum longus; FHL, flexor hallucis longus; HyperPP, hyperkalemic periodic paralysis; HypoPP, hypokalemic periodic paralysis; LET, long exercise test; MRI, magnetic resonance imaging; mRS, modified Rankin Scale; NHS, National Health Service; PP, periodic paralyses; RF, rectus femoris; SD, standard deviation; STIR, short tau inversion recovery; TA, tibialis anterior.

Tarek Yousry and Michael G. Hanna are joint senior authors.

This is an open access article under the terms of the [Creative Commons Attribution-NonCommercial-NoDerivs](https://creativecommons.org/licenses/by-nc-nd/4.0/) License, which permits use and distribution in any medium, provided the original work is properly cited, the use is non-commercial and no modifications or adaptations are made.

© 2023 The Authors. *Muscle & Nerve* published by Wiley Periodicals LLC.

## KEYWORDS

channelopathies, hyperkalemic, hypokalemic, MRI, periodic paralysis

## 1 | INTRODUCTION

The periodic paralyses (PP) are a group of genetic conditions including hypokalemic PP (hypoPP), hyperkalemic PP (hyperPP), and Andersen-Tawil syndrome (ATS). The minimum point prevalence for hypoPP and hyperPP is  $0.41 \times 10^{-5}$  and  $0.1 \times 10^{-5}$  for ATS.<sup>1</sup> They are all due to dysfunction of voltage-gated ion channels in skeletal muscle. The clinical effect is muscle weakness or paralysis. The muscle symptoms may be episodic weakness, episodic with fixed weakness, or progressive fixed weakness.

Muscle magnetic resonance imaging (MRI) has been used in several neuromuscular conditions for diagnosis and monitoring.<sup>2</sup> Characteristic patterns of involvement can be seen, which can then direct more targeted genetic testing or research level testing.<sup>3</sup> In addition, we previously demonstrated that fat fraction quantitation correlates with disability in two neuromuscular diseases.<sup>2,4</sup> There are few studies of MRI in the PP.<sup>5-9</sup>

This study aims to compare all subsets of PP with systematic evaluation of intramuscular fat accumulation, atrophy, and STIR hyperintensity on MRI. We aimed to identify the pattern of MRI involvement in patients with hypoPP, hyperPP, and ATS and compare MRI changes to healthy controls. We compared MRI findings with detailed clinical features and in relation to treatments.

## 2 | METHODS

### 2.1 | Participants

Patients with a genetically confirmed diagnosis of hypoPP, hyperPP, or ATS had lower limb muscle MRI scans performed between the years 2008 and 2019 as part of a cohort study. All consecutive patients with MRI scans were reviewed in this retrospective cohort study. Patients with *SCN4A* mutations could also have myotonia but had a predominant hyperPP phenotype. Participants were part of a cohort study (Investigation of human neurological ion channel or episodic neurological disorders, REC 07/Q0512/2), which has ethics approval from the Joint National Hospital for Neurology and Institute of Neurology Research Ethics Committee. Written informed consent was obtained for the MRI scans as well as collection of retrospective clinical data. Eight healthy volunteers were also enrolled to the MRI in Channelopathies study (REC Ref: LO/11/1800) which has Ethics approval from the Joint National Hospital for Neurology and Institute of Neurology Research ethics Committee. This separate study attained ethics approval to enroll healthy volunteers. Control participants were recruited from staff and relatives/associates of staff at our institution. Prior to their MRI, all healthy volunteers underwent a medical history and focused clinical examination to exclude any

participants with other factors that would affect lower limb MRI (e.g., injuries affecting lower limb muscles). Clinical details for patients were obtained retrospectively from review of their National Health Service (NHS) medical records: sex, age at scan, year of scan, symptom onset, treatment for weakness and treatment dose, treatment duration, need for additional medication, use of a gait aid, presence of weakness defined as Medical Research Council grade 4 or lower in any major muscle group, pattern of weakness, presence of discrete attacks of weakness within 5 y of the MRI scan, and amplitude decrement on long exercise test.

The participant's level of disability at the time of the MRI scan was scored using the modified Rankin Scale (mRS) (supplement).<sup>10</sup>

### 2.2 | MRI protocol

Participants underwent 3 T MRI (Siemens TIM Trio, Erlangen, Germany) examination of the lower limb muscles. A routine imaging protocol was utilized, comprised of axial T1-weighted and axial short-tau-inversion-recovery (STIR) sequences of both thighs and both calves with 5 mm slice thickness and 1 mm slice gap. The total time required for the MRI examination was less than 20 min.

The acquired images were reviewed by a radiologist with expertise in neuromuscular MRI (S.S.). The reader was given the age of the patient, but blinded to all other details including disease status. A total of 18 muscles were assessed bilaterally: rectus femoris, vastus intermedius, vastus lateralis, vastus medialis, semimembranosus, semitendinosus, biceps femoris, adductor magnus, adductor longus, gracilis and sartorius in the thigh; tibialis anterior, extensor hallucis longus/extensor digitorum longus, peroneal longus/brevis, medial gastrocnemius, lateral gastrocnemius, soleus, and tibialis posterior in the calf.

Each muscle was scored individually on the T1-weighted sequences for the presence of fat accumulation using the six-point Mercuri scale.<sup>11</sup> Atrophy was scored by neuromuscular MRI experts based on assessment of the cross-sectional area of a muscle, compared to the contralateral side or other muscle groups.<sup>12,13</sup> Water deposition was assessed on the STIR sequences using a semi-quantitative scale for the severity and extent of hyperintensity. The scales are detailed below. Pelvic muscles were not formally scored; however, they were reviewed and a comment noted if fat accumulation was present.

- Fat accumulation
  - 0 – normal appearance
  - 1 – early fat accumulation with scattered areas of T1 high signal
  - 2 – numerous discrete areas of T1 high signal with beginning confluence <30% of the total muscle volume
  - 3 – fat accumulation 30–60% of the muscle volume

- 4 – fat accumulation >60% of the muscle volume
- 5 – end-stage, no residual muscle tissue
- Muscle atrophy
  - 0 – no atrophy
  - 1 – minimal, <30% of the muscle volume
  - 2 – moderate atrophy, >30% and <60% of the muscle volume
  - 3 – severe atrophy, >60% of the muscle volume
- STIR extent
  - 0 – no edema
  - 1 – minor extent, <30% of the muscle volume
  - 2 – 30% to 60% of the muscle volume
  - 3 – major extent, >60% of the muscle volume
- STIR intensity
  - 0 – normal intensity
  - 1 – mild hyperintensity
  - 2 – severe hyperintensity

Ten percent of the MRI examinations were selected randomly and additionally reviewed by a second radiologist with expertise in neuromuscular imaging, who was also blinded to clinical details (T.Y.). An average concordance of 91% was seen across all domains. This was deemed acceptable, and the first reviewer's scores were used.

### 2.3 | Statistical analysis

Aside from analysis of asymmetry, all other statistics and figures used the mean score of left and right muscles.

For baseline data, mean and standard deviation (SD) were used for normally distributed data and median and range for data that were not normally distributed. Categorical variables were expressed as

counts and percentages. Means were compared by using the independent t test. Proportions for categorical variables were compared using the  $\chi^2$  test. Correlation analysis was performed using a Spearman correlation. Strong or very strong correlations were defined as 0.70–1.00, moderate correlations as 0.40–0.69 and weak correlations as 0.10–0.39.<sup>14</sup> All statistical analyses were performed using SPSS Statistics version 22 (IBM, Armonk, NY) and Excel version 16.41 (Microsoft, Redmond, WA). The significance threshold was set at a two-sided *P*-value less than 0.05.

## 3 | RESULTS

A total of 45 patients and eight controls were included in the study (Table 1): 20 families with hypoPP, 9 with hyperPP, and 8 with ATS. Three patients of those with *SCN4A* variants had a hypoPP phenotype. Characteristics are described in Table 1. Thirty-one patients (69%) had weakness on clinical examination.

Six patients did not have discrete attacks of paroxysmal weakness within 5 y of undertaking the MRI. Four of these patients had hypoPP and had rare attacks early in life before developing a slowly progressive myopathy with marked weakness. The other two patients had ATS: one with no muscle symptoms and the other with generalized fatigue. Both patients with ATS had some evidence of fat accumulation on MRI as well as pelvic muscle involvement.

A total of 28 patients had long exercise testing (LET) (Table 1); 11 patients had a negative LET. Of these 11, 5 had episodic weakness and fixed weakness, 4 patients had episodic weakness and no fixed weakness, and 2 patients had neither episodic or fixed weakness. There was no major difference in LET decrement between sex.

**TABLE 1** Participant characteristics.

	All patients	<i>CACNA1S</i>	<i>SCN4A</i>	<i>KCNJ2</i>	Controls
No. of subjects	45	17	16	12	8
Age mean (SD) (y)	42 (13)	40 (15)	42 (13)	45 (10)	43 (14)
Age range (y)	18–72	18–72	18–63	25–60	27–63
Male	31 (69.8%)	12 (70.6%)	11 (68.8%)	8 (66.7%)	5 (62.5%)
MRS mean (SD)	2.4 (1.1)	2.5 (0.9)	2.3 (1)	2.3 (1.4)	0
MRS 0 (n)	1	0	0	1	8
MRS 1 (n)	9	2	4	3	0
MRS 2 (n)	16	8	5	3	0
MRS 3 (n)	11	4	5	2	0
MRS 4 (n)	8	3	2	3	0
MRS 5 (n)	0	0	0	0	0
No. of patients with a positive LET	17 (60.7%)	5 (62.5%)	5 (55.6%)	7 (63.6%)	
Most common mutation (n)		Arg1239His (9)	Thr704Met (7)	Arg312Cys (4)	
On treatment	42 (93%)	17 (100%)	15 (94%)	10 (83%)	0
Need of a gait aid	9 (20%)	3 (18%)	2 (13%)	4 (33%)	0
Weakness on examination	31 (69%)	12 (71%)	10 (63%)	9 (75%)	0

Abbreviations: LET, long exercise test; MRS, modified Rankin Scale.

The most commonly used treatment was acetazolamide, which was taken by 23 patients (52%). This was followed by dichlorphenamide (7 patients;17%), amiloride (6 patients;14%), mexiletine (2 patients; 4%), and salbutamol (1 patient; 2%). The average treatment duration was 4.4 y (SD 5.7). Thirty-four patients (76%) required more than one medication. The most commonly used add-on medication was potassium supplementation followed by amiloride.

### 3.1 | Fat accumulation

Of 45 patients, 35 (78%) had an abnormal MRI scan. In 2 of 8 controls, mild fat accumulation was seen in three muscles (adductor magnus, biceps femoris, or soleus). When compared to controls, patients with periodic paralysis had more fat accumulation (*SCN4A*  $P = .0006$ ; *CACNA1S*  $P = .01$ ; *KCNJ2*  $P = .02$ ).

The most affected muscles in patients were adductor magnus in the thigh and medial gastrocnemius in the calf (Figure 1). Patients with *SCN4A* variants were most severely affected with a mean Mercuri score of 1.3, compared to a mean Mercuri score of 0.7 for patients with *CACNA1S* variants and 0.3 for patient with *KCNJ2* variants. This is also illustrated by the clustering of patients with *SCN4A* variants in the heat map (Figure 1).

Generally, patients with the greatest disability determined by MRS score had the greatest intramuscular fat accumulation. However, four outliers were noted (Figure 1), having high disability scores (MRS 3 or 4) but with minimal fat accumulation across all thigh and calf muscles. Three of these patients harbored *KCNJ2* variants. Two patients had proximal pelvic muscle fat accumulation.

Patients with *SCN4A* variants had the greatest degree of fat accumulation. In the thigh, adductor magnus and sartorius had greatest involvement with relative sparing of vastus intermedius and adductor longus (Figure 2). In the calf, the superficial posterior compartment muscles were most affected, most notably gastrocnemius medialis. Patients with *KCNJ2* variants had lesser fat accumulation overall, with biceps femoris and medial gastrocnemius the most affected muscles in thigh and calf, respectively. Patients with *CACNA1S* variants had an intermediate degree of fat accumulation with the posterior muscles showing greater involvement in the calf, and adductor magnus the most affected muscle in the thigh.

There was no statistically significant difference between the degree of fat accumulation seen in the thigh versus the calf muscles in any group (*SCN4A* diff 0.25,  $P = .56$ ; *CACNA1S* diff 0.24,  $P = .49$ ; *KCNJ2* diff 0.004,  $P = .98$ ). The pelvic muscles were affected in 28 patients (62%), evenly spread across the subgroups.

Four patients had progressive myopathy with no attacks of weakness within 5 y of the MRI scan. These patients were the most severely affected (assessed by MRI Mercuri score) patients of the cohort (Figure 1).

In eight patients, left–right asymmetry in fat accumulation was seen in one or more muscles by two or more Mercuri points. A difference of four points in semimembranosus was seen in two of these patients with *SCN4A* mutations. A further 15 patients had minor left–right asymmetry in one muscle by one Mercuri point.

### 3.2 | Muscle atrophy

Atrophy was not seen in any control participants. Overall, atrophy was a mild feature of the cohort. The overall mean atrophy score was 0.1. 42% of patients had no muscle atrophy.

Only 12 patients had a sum atrophy score greater than or equal to 2, but the average atrophy score was still low. Eight of these patients carried *SCN4A* variants and corresponded to those with more severe fat accumulation. The most affected patient had a sum muscle atrophy score of 12.5 but still a low average atrophy score. The most affected muscle was adductor magnus.

### 3.3 | STIR intensity

Only one control participant had mildly increased STIR hyperintensity in the posterior calf muscles. Of 45 patients, 30 (67%) had STIR hyperintensity in at least one muscle. Vastus lateralis was the most affected muscle in the thigh, and medial and lateral gastrocnemius were the most affected in the calf (Figure 3).

The more severely affected patients, as assessed by STIR intensity changes, were those with *SCN4A* and *CACNA1S* variants, with clustering demonstrated in Figure 3. Three outliers were noted – with no STIR hyperintensity in any muscles but disability score of MRS 3 or 4. These three patients all harbored *KCNJ2* variants. Pelvic muscle fat accumulation was noted in these patients.

The pattern of STIR hyperintensity was similar in *SCN4A* and *CACNA1S* with the anterior thigh and posterior calf predominantly affected. STIR hyperintensity was not a predominant part of the MRI pattern of *KCNJ2* (Figure 4).

A pattern of peri-tendinous STIR hyperintensity was seen in nine patients (Figure 5). This was identified in one patient and then assessed systematically in all participants. Of all patients with STIR hyperintensity in tibialis anterior (TA), five (21%) demonstrated concentric STIR hyperintensity around the TA tendon on multiple slices. Three patients carried *SCN4A* variants; one *CACNA1S* and one *KCNJ2*. Similar peri-tendinous STIR hyperintensity was seen in rectus femoris (RF) in three patients (16% of all patients with RF STIR hyperintensity) (Figure 5). All three patients harbored different variants. This pattern of involvement was also seen in one patient in extensor digitorum longus (EDL) and another in flexor hallucis longus (FHL). Seven of these nine patients had fixed weakness on clinical examination. MRS disability scores varied from 0 to 3. These seven patients were all on treatment. The remaining two patients, both with *KCNJ2* variants, had no episodic or fixed weakness.

### 3.4 | Correlations

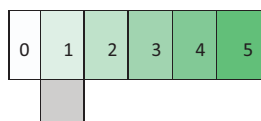
An average Mercuri score of 0.77 (SD 1.2) was seen for females versus 0.82 (SD 1.0) for males, a difference that was not statistically significant ( $P = .89$ ).

A weak Spearman rank correlation between disability (using the MRS score) and Mercuri scores was seen ( $r = 0.35$ ;  $P = .02$ ), as well

Gene	MRS Score	Fixed weakness	Thigh Muscles										Calf Muscles						Mean Mercuri	Mean Atrophy	Pelvic Involvement	Mean STIR		
			Add. Magnus.	Sartorius	B. Femoris	V. Lateralis	V. Medialis	Semimembranosus	Semitendinosus	R. Femoris	V. Intermedius.	Gracilis	Add. Longus	Gastroc. Medialis.	Soleus	Gastroc. Lateralis.	P. Longus	Tib. Anterior					Tib. Post	EHL/EDL
KCNJ2*	3	Yes	0	0	0	0	0	0	0	0	0	0	0	0	0	0	0	0	0	0	0.00	0.0	No	0
SCN4A	1	No	0	0	0	0	0	0	0	0	0	0	0	0	0	0	0	0	0	0	0.00	0.0	No	0.0
CACNA1S	1	No	0	0	0	0	0	0	0	0	0	0	0	0	0	0	0	0	0	0	0.00	0.0	No	0.0
CACNA1S	2	No	0	0	0	0	0	0	0	0	0	0	0	0	0	0	0	0	0	0	0.00	0.0	No	0.0
KCNJ2	1	Yes	0	0	0	0	0	0	0	0	0	0	0	0	0	0	0	0	0	0	0.00	0.0	No	0.16667
CACNA1S	2	No	0	0	0	0	0	0	0	0	0	0	0	0	0	0	0	0	0	0	0.00	0.0	No	0.0
CACNA1S	2	Yes	0	0	0	0	0	0	0	0	0	0	0	0	0	0	0	0	0	0	0.00	0.0	No	0.05556
CACNA1S	1	No	0	0	0	0	0	0	0	0	0	0	0	0	0	0	0	0	0	0	0.00	0.0	Yes	0.0
SCN4A	2	No	0	0	0	0	0	0	0	0	0	0	0	0	0	0	0	0	0	0	0.00	0.0	Yes	0.0
KCNJ2	2	No	0	0	0	0	0	0	0	0	0	0	0	0	0	0	0	0	0	0	0.00	0.0	Yes	0.02778
CACNA1S	2	Yes	1	0	0	0	0	0	0	0	0	0	0	0	0	0	0	0	0	0	0.06	0.1	No	0.33333
KCNJ2*	4	Yes	0.5	0	0	0	0	0.5	0	0	0	0	0	0	0	0	0	0	0	0	0.06	0.0	Yes	0.0
SCN4A*	3	Yes	0	0	0	0	0	0	0	0	0	0	0	1	0	0	0	0	0	0	0.06	0.1	No	0.05556
KCNJ2*	4	Yes	0	0	1	0	0	0	0	0	0	0	0	0.5	0	0	0	0	0	0	0.08	0.0	Yes	0.05556
SCN4A	1	No	0	1.5	0	0	0	0	0	0	0	0	0	0.5	0	0	0	0	0	0	0.11	0.1	No	0.13889
KCNJ2	2	Yes	0	1	0	0	0	0	0	0	0	0	0	0	0	0	1	0.5	0	0	0.14	0.0	Yes	0.0
CACNA1S	3	Yes	0	0	0	0	0	0	0	0.5	0	0	0	1	1	0	0	0	0	0	0.14	0.0	Yes	0.69444
KCNJ2	1	No	0	0.5	0	0	0	0.5	0	0	0	0	0	1	1	0	0	0	0	0	0.17	0.0	Yes	0.16667
KCNJ2	4	Yes	0	1	1	0	0	0	0	0	0	1	0	0	0	0	0	0	0	0	0.17	0.0	No	0
CACNA1S	3	Yes	1	0	0	1.5	1	0	0	0	0	0	0	0	0	0	0	0	0	0	0.19	0.0	Yes	0.5
SCN4A	1	No	0	0.5	1	0	0	1	0	0	0	0.5	0	0	0.5	0	0	0	0	0	0.19	0.0	No	0.08333
KCNJ2	2	Yes	0	1	1	0	0	0	0	0	0	0	0	2	0	0	0	0	0	0	0.22	0.0	No	0.05556
CACNA1S	2	Yes	1	1	1	0	0	1	1	0	0	1	0	0	0	0	0	0	0	0	0.33	0.0	No	0.0
SCN4A	2	Yes	1	1.5	1	0	0	1	1	0	0	1	0	1	0	0	0	0	0	0	0.42	0.0	Yes	0.47222
CACNA1S	4	Yes	1	1	0	1	1	0	0	0.5	1	0	0	1	0.5	0	0	0	1	0	0.44	0.4	Yes	1.16667
CACNA1S	2	No	1	1	1	0	0	1	1	0	0	1	0	0	0	0	1	1	0	1	0.50	0.0	Yes	0.41667
CACNA1S	2	Yes	1	1	1	0	0	1	1	0	0	0	0	1	0	0	1	1	1	1	0.56	0.0	Yes	0.30556
KCNJ2	3	Yes	1	1	1	0	0	1	1	0	0	0	0	2.5	2	0.5	1	0	0	0	0.61	0.1	Yes	0.13889
SCN4A	3	Yes	1	1	1	0	0	1	1	1	0	1	0	1.5	0.5	1	0	0.5	0.5	0	0.61	0.1	Yes	0.22222
SCN4A	2	Yes	2.5	2	0	0	0	0	0	2	0	2	0	2	1	1	0	0	0	0	0.69	0.2	Yes	0.30556
KCNJ2	1	Yes	1	0	4	0	0	4	1	0	0	0	1	1	1	0	1.5	0	0	0	0.81	0.0	Yes	0.02778
KCNJ2	0	No	0.5	1	1	1	1	1	1	0.5	1	1	1	1	1	1	0	1	1	1	0.89	0.1	Yes	0.02778
CACNA1S	2	Yes	1	1	1	2	2	1	3	1	0	1	0	2.5	1	1	0.5	0	0	0	1.00	0.1	Yes	0.38889
CACNA1S	3	Yes	1	3	1	0.5	0.5	1	1.5	0.5	0.5	1	1	1	2	0	1	1	1	1	1.03	0.2	Yes	0.27778
SCN4A	2	Yes	2	1	2	1	1	1	1	1	0	1	0	2	2	0.5	3	1	1	1	1.25	0.2	Yes	0.27778
SCN4A	3	Yes	3	4	0.5	2.5	2.5	0	0	2	1.5	1.5	0	4	1	4	0	0	0	0	1.47	0.7	No	0.44444
CACNA1S	3	Yes	4	0	2.5	4	3.5	2.5	2	0	2	0	1	1	2.5	1	1	0.5	2	0.5	1.67	0.4	Yes	0.58333
SCN4A	2	No	4	2	4	3	3.5	2	3.5	1	1	1	0	4	3	4	0.5	0	0	0	2.03	0.2	Yes	0.5
SCN4A	1	No	4	4	1	3	3	1	1.5	3	0	2	4	2	5	1.5	2	0	0	0	2.18	0.4	Yes	0.84375
SCN4A	3	Yes	4	4	3	3	4	5	4	1	2.5	2	2	4	2	2	1	1	1.5	1	2.61	0.2	Yes	1.20588
SCN4A	3	Yes	4	4	2.5	4	3.5	0	1.5	4	3.5	1	0	5	4	4	2	3	1	3	2.78	0.6	Yes	1.05882
SCN4A**	4	Yes	4	2	3	1	2	1.5	2	4	1	4	4	4	4	2	4	4	2	4	2.92	0.4	No	0.55556
CACNA1S**	4	Yes	4	2	4	4	5	5	3	2.5	4	2	3	5	4	2	1	2	3.5	0	3.11	0.0	No	0.46667
CACNA1S**	4	Yes	5	3	3.5	5	5	5	3	3	5	1	2.5	4.5	4	3	1	2	3.5	0	3.28	0.6	Yes	0.05556
SCN4A**	4	Yes	5	3.5	3.5	3	3.5	3	3.5	3	2.5	3.5	4								3.45	0.8	Yes	1.11111
Mean	2.4		1.3	1.1	1.0	0.9	0.9	0.9	0.8	0.7	0.6	0.6	0.5	1.2	0.9	0.7	0.5	0.4	0.4	0.3	0.79	0.1		

Key

Mercuri scores



Unable to be Scored

**FIGURE 1** Heat map of Mercuri scores for fat accumulation, stratified by mean Mercuri score. Most severely affected patients appear towards the bottom; most severely affected muscles (darker green) on the left within the thigh and calf separately. mRS, modified Rankin Scale; \*, patients with mismatch between MRS disability score and MRI Mercuri score; \*\*, patients with a progressive myopathy phenotype without attacks.

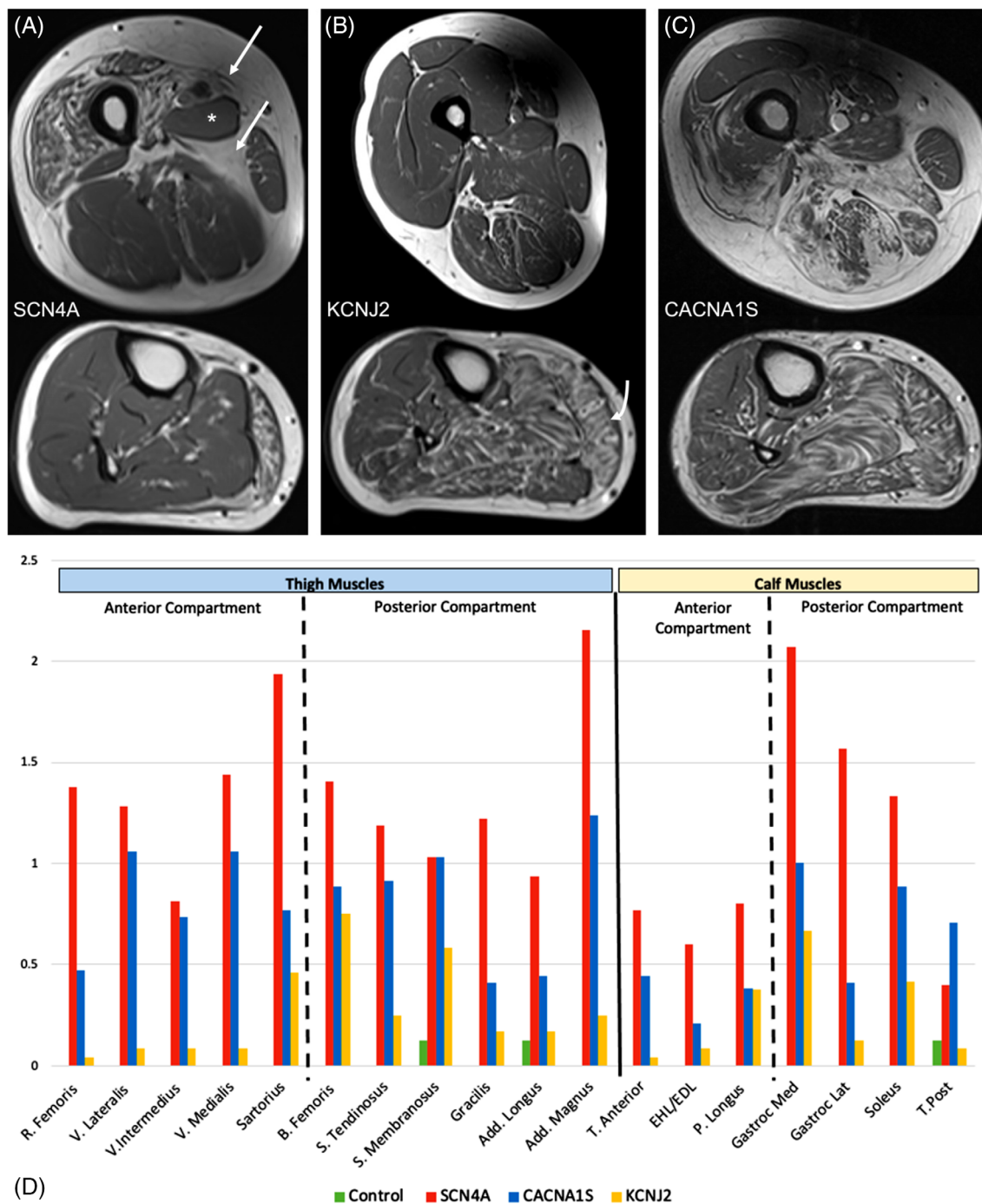


**FIGURE 2** (A–C) Representative T1w muscle MRI appearances. (A) Axial T1-weighted images of the thigh muscles (top panel) and calf muscles (bottom panel), illustrating patients with *SCN4A* mutations having a predisposition for fat accumulation within the anterior thigh and superficial posterior calf muscles, with particular involvement of sartorius and adductor magnus (arrows) and sparing of adductor longus (asterisk). (B) Patients with *KCNJ2* mutations have less marked intramuscular fat accumulation in the thigh, although involvement of the posterior calf muscles is seen, particularly medial gastrocnemius (curved arrow). (C) The pattern of thigh muscle involvement in patients with *CACNA1S* mutations is less selective, although there is predominant involvement of the posterior calf muscles. (D) Bar chart demonstrating mean Mercuri scores (y axis) for each muscle, grouped by gene.

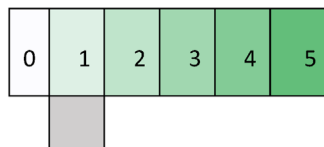
as between disability and atrophy ( $r = 0.32$ ,  $P = .03$ ) and between disability and STIR hyperintensity ( $r = 0.30$ ,  $P = .03$ ) (Figure 6A). Mercuri scores increased (moderate correlation) with increasing STIR intensity scores ( $r = 0.69$ ,  $P = 1.50 \times 10^{-7}$ ).

A moderate correlation was seen between Mercuri scores and age for *SCN4A* and *CACNA1S* ( $r = 0.47$ ,  $P = 0.02$ ) (Figure 6B). Those with *SCN4A* and *CACNA1A* variants developed more intramuscular fat accumulation with age. This trend with age was not seen in patients

Gene	MRS Score	Thigh Muscles											Calf Muscles					Mean STIR	Mean Mercuri	Mean Atrophy				
		V. lateralis	V. Medialis	V. Intermedius	R. Femoris	B. Femoris	S. Membranosus	Add. Magnus	Sartorius	S. Tendinosus	Gracilis	Add. Longus	Gastroc Med	Gastroc Lat	Soleus	T. Anterior	EHU/EDL				P. Longus	T. Post		
KCNJ2	3	0	0	0	0	0	0	0	0	0	0	0	0	0	0	0	0	0	0	0	0	0.00	0.0	0.0
SCN4A	1	0	0	0	0	0	0	0	0	0	0	0	0	0	0	0	0	0	0	0	0	0.00	0.0	0.0
KCNJ2	2	0	0	0	0	0	0	0	0	0	0	0	0	0	0	0	0	0	0	0	0	0.00	0.1	0.0
CACNA1S	1	0	0	0	0	0	0	0	0	0	0	0	0	0	0	0	0	0	0	0	0	0.00	0.2	0.0
KCNJ2	4	0	0	0	0	0	0	0	0	0	0	0	0	0	0	0	0	0	0	0	0	0.00	0.4	0.4
CACNA1S	2	0	0	0	0	0	0	0	0	0	0	0	0	0	0	0	0	0	0	0	0	0.00	0.0	0.0
CACNA1S	2	0	0	0	0	0	0	0	0	0	0	0	0	0	0	0	0	0	0	0	0	0.00	0.4	0.0
KCNJ2	4	0	0	0	0	0	0	0	0	0	0	0	0	0	0	0	0	0	0	0	0	0.00	0.9	0.1
CACNA1S	1	0	0	0	0	0	0	0	0	0	0	0	0	0	0	0	0	0	0	0	0	0.00	1.0	0.2
CACNA1S	2	0	0	0	0	0	0	0	0	0	0	0	0	0	0	0	0	0	0	0	0	0.00	3.5	0.8
SCN4A	2	0	0	0	0	0	0	0	0	0	0	0	0	0	0	0	0	0	0	0	0	0.00	3.3	0.6
KCNJ2	1	0	0	0	0	0	0	0	0	0	0	0	0	0	0	0	0	0	0	0	0	0.03	0.8	0.0
KCNJ2*	0	0	0	0	0.5	0	0	0	0	0	0	0	0	0	0	0	0	0	0	0	0	0.03	0.1	0.0
KCNJ2*	2	0	0	0	0	0	0	0	0	0	0	0	0	0	0	0	0	0	0	0	0	0.03	0.8	0.1
KCNJ2	4	0	0	0	0	0	0	0	0	0	0	0	1	0	0	0	0	0	0	0	0	0.06	0.1	0.0
KCNJ2	2	0	0	0	0	0	0	0	0	0	0	0	1	0	0	0	0	0	0	0	0	0.06	0.2	0.0
CACNA1S	2	0	0	0	0	0	0	0	0	0	0	0	0	0	0.5	0	0	0	0	0	0	0.06	2.8	0.6
CACNA1S	4	0	0	0	0	0.5	0	0	0	0	0	0	0	0	0	0	0.5	0	0	0	0	0.06	0.7	0.2
SCN4A	3	0	0	0	0	0	0	0.5	0	0.5	0	0	0	0	0	0	0	0	0	0	0	0.06	1.0	0.1
SCN4A*	1	0	0	0	0	0	0	0	0	0	0	0	0.5	0.5	0	0.5	0	0	0	0	0	0.08	0.0	0.0
SCN4A*	1	0	0	0	0	0	0	0	0	0.5	0	0	1	1	0	0	0	0	0	0	0	0.14	0.1	0.1
KCNJ2	3	0	0	0	0	0	0	0	0	0	0	0	1	0.5	0.5	0	0	0.5	0	0	0	0.14	0.6	0.1
KCNJ2	1	0	0	0	0	0	0	0	0	0	0	0	1	0	1	0.5	0.5	0	0	0	0	0.17	0.2	0.0
KCNJ2	1	0	0	0	0	0	0	0	0	0	0	0	1	1	0	0	0.5	0	0.5	0	0.5	0.17	0.2	0.0
SCN4A	3	0	0	0	0	0	0	0	0	0	0	0	1	1	0.5	0.5	1	0	0	0	0	0.22	0.3	0.0
SCN4A*	2	0	0.5	0	0	0	0	0.5	0	0	0	0.5	0	0.5	1	1	1	0	0	0	0	0.28	1.3	0.2
CACNA1S	3	1	0.5	0.5	0	0	0	0	0.5	0	0	0	1	0	0.5	0.5	0.5	0	0	0	0	0.28	2.6	0.2
SCN4A*	2	1	0	0	0.5	0	0	0	0	0	0	0	1	1	1.5	0	0	0.5	0	0	0	0.31	0.6	0.0
CACNA1S	2	0	0	0.5	0.5	0	0	0	0	0	0	1	0	1	1	0	0.5	0.5	0.5	0	0	0.31	1.5	0.7
CACNA1S*	2	0	0	0	0	0.5	0.5	0	0	0	0	0	1	2	1	1	0	0	0	0	0	0.33	0.1	0.1
CACNA1S*	2	2	0	1	1	0	0	1	0	0	0	0	0	1	0.5	0	0	0.5	0	0	0	0.39	0.0	0.0
CACNA1S	2	0	0	0	0	0.5	0	0	0	0	0	0	1	1	1	1	1	1	1	1	1	0.42	0.6	0.1
SCN4A	3	2	1.5	1	1	0	0	0	0	0	0	0	0	0	1	0.5	0	0	1	0	1	0.44	1.7	0.4
CACNA1S	4	1.5		0	0.5	0		0	0	0	0	0		1	1	1	1	1	1	0	0.47	3.1	0.0	
SCN4A	2	1	1	1	1	0.5	0	0.5	0	0	1	0	0	1	0.5	0.5	0	0.5	0	0	0	0.47	0.1	0.0
SCN4A	2	1	1	1	0	1	1	0	1.5	0	0.5	0	0	0	0.5	0.5	0.5	0.5	0	0	0	0.50	2.0	0.2
CACNA1S	3	1	1	1	1	0	0.5	0	0	0	0	0	1	0.5	0.5	0.5	0.5	1.5	0	0	0	0.50	0.2	0.0
SCN4A	4	0.5	1	0.5	0.5	0	0	0	0	0	0	0.5	1	1	1	1	1	1	1	1	1	0.56	0.5	0.0
CACNA1S	3	1	1.5	1	0.5	1	1	1	0	0	0	0	1	1	1	0.5	0	0	0	0	0	0.58	0.1	0.1
CACNA1S	3	1	1	1	1	0	0.5	0	0.5	0.5	0	1	0	0	0.5	1.5	2	2	0	0	0	0.69	0.80	0.13
CACNA1S	3	1	1	1	1	0.5	0.5	1	0	0	0.5	0	1.5	2	2	0	0	0.5	0	0	0	0.69	0.0	0.0
SCN4A	1	1.5	1.5	0	1	1	1	0.5	0	2	1	0.5			1	1	0.5	1	0	0	0.84	2.2	0.4	
SCN4A*	3	2	2	2	1	2	1	0	1	0.5	0	0		1	2	1	1	1	0.5	0	1.06	0.0	0.0	
SCN4A	4	2	2	1	1	1	1		0.5	0.5	1										1.11	0.0	0.0	
CACNA1S	4	2	2	2	1	1	1	1	1	0.5	1	0	1	2	1	1	1.5	1	1	1	1.17	0.0	0.0	
SCN4A	3	2	2	1	1	1	1		1	2	1	1	1	1	1	1.5	1	1	1	1	1.21	2.9	0.4	
Average	2.11	0.51	0.43	0.34	0.30	0.23	0.18	0.16	0.15	0.15	0.13	0.08	0.48	0.48	0.47	0.36	0.33	0.31	0.13	0.30	0.82	0.14		

Key

Mercuri scores



Unable to be Scored

**FIGURE 3** Heat map of STIR hyperintensity scores, stratified by mean STIR score. Most severely affected patients appear at the bottom; as well as most severely affected muscle (darker green) on the left within the thigh and calf compartments. mRS, modified Rankin Scale; \*, patients with peri-tendinous STIR hyperintensity.

with KCNJ2 variants. While fat accumulation increased with increasing age, most young patients had fat accumulation on MRI: 12/16 patients under 40 had fat accumulation on MRI.

Further correlations were not seen between Mercuri scores and disease onset, treatment duration or decrement on long exercise testing. Controlling for age, no statistically significant correlation was seen

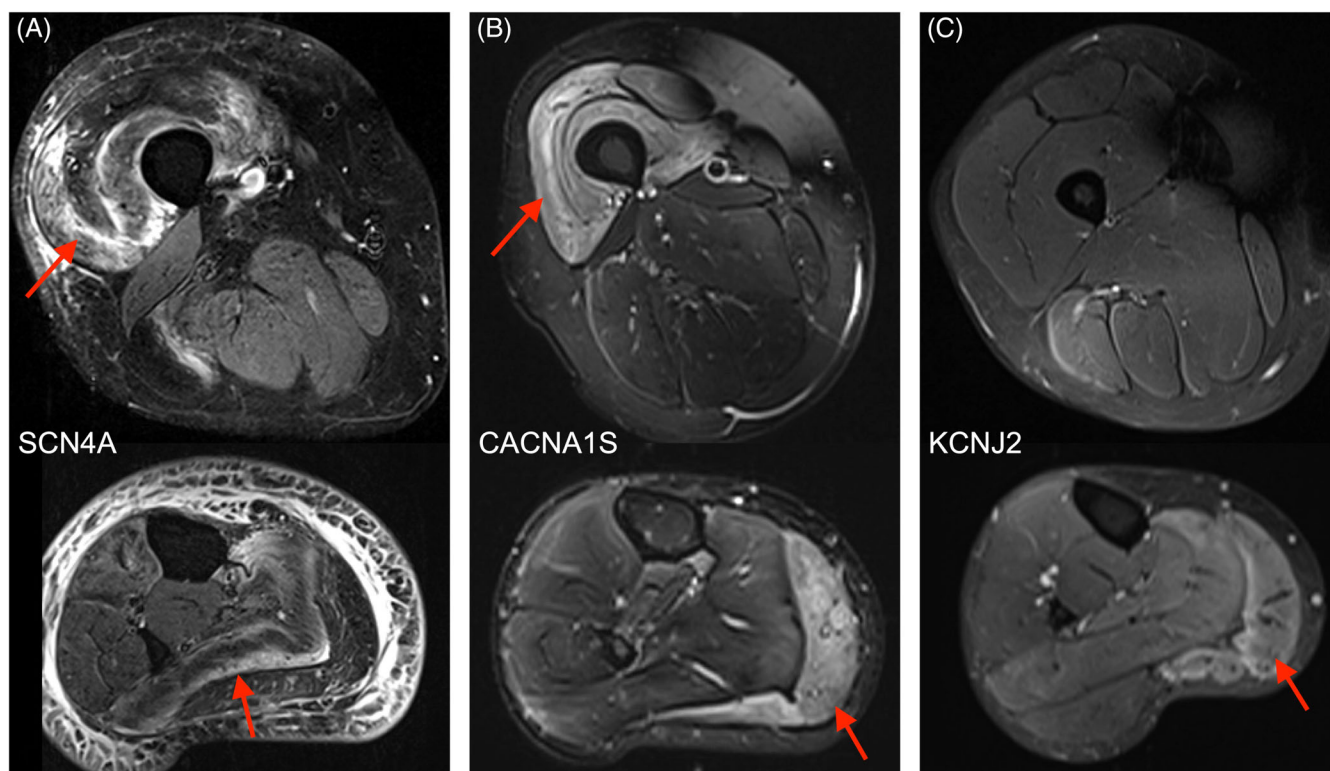


**FIGURE 4** Representative STIR muscle MRI appearances. Axial STIR images of the thigh muscles (top panel) and calf muscles (bottom panel), demonstrating that patients with (A) *SCN4A* and (B) *CACNA1S* mutations have a predisposition for water deposition affecting the anterior thigh and posterior calf muscles, whereas patients with (C) *KCNJ2* mutations show minimal thigh involvement but predominant involvement of the posterior calf muscles (arrow = muscles most affected by described increased STIR signal).

between Mercuri scores and age of symptom onset or treatment duration. No statistically significant correlation was seen between STIR hyperintensity and symptom onset, treatment duration, or decrement on LET.

A total of 14 patients did not have any fixed weakness on clinical examination. Seven of these patients had fat accumulation on MRI (for these seven patients – average Mercuri score 0.15 [SD 0.1]; average STIR score 0.29 [SD 0.3]).

Six patients had STIR hyperintensity with no fat accumulation. The average age of these patients was 42 y, compared to an average age of patients with fat accumulation of 46 y.

In patients with hyperPP and hypoPP, there was no statistically significant difference in STIR hyperintensity between those who had episodic weakness and those with a progressive myopathy phenotype.

## 4 | DISCUSSION

We demonstrated significant fat accumulation and STIR hyperintensity in patients with PP. The most severe fat accumulation was seen in those with *SCN4A* variants. We observed different degrees of thigh involvement depending on the gene involved: in patients with *SCN4A* variants, a pattern of involvement on T1-weighted sequences most

affected the adductor magnus and sartorius in the thigh; in contrast, patients with *KCNJ2* exhibited greater hamstring involvement, whereas thigh muscles in patients with *CACNA1S* showed less selective involvement. In addition, we observed a distinctive peri-tendinous STIR hyperintensity in some patients, not seen in other genetic myopathies. We identified weak to moderate correlations between Mercuri scores and STIR hyperintensity as well as between Mercuri score and age for patients with *SCN4A* and *CACNA1S* variants.

Previous MRI studies have focused on particular PP subgroups. Similar to our study, a study of HypoPP patients harboring the same mutation (Arg528His) in *CACNA1S* reported evidence of fat accumulation in muscle of patients with no fixed weakness.<sup>7</sup> One study of seven patients with hyperPP (Thr704Met) described intramuscular fat accumulation, worse in older patients.<sup>9</sup>

### 4.1 | Significant myopathy and disability

In our cohort, disability as well as corresponding fat accumulation on MRI increased with age. It is important to note that this process can start early – 75% of patients under 40 y (range 18–40) had fat accumulation on MRI. Our findings support two previous smaller reports that describe a subset of patients with fixed weakness and disability at younger ages.<sup>7,15</sup> In our series, two-thirds of patients had clinical



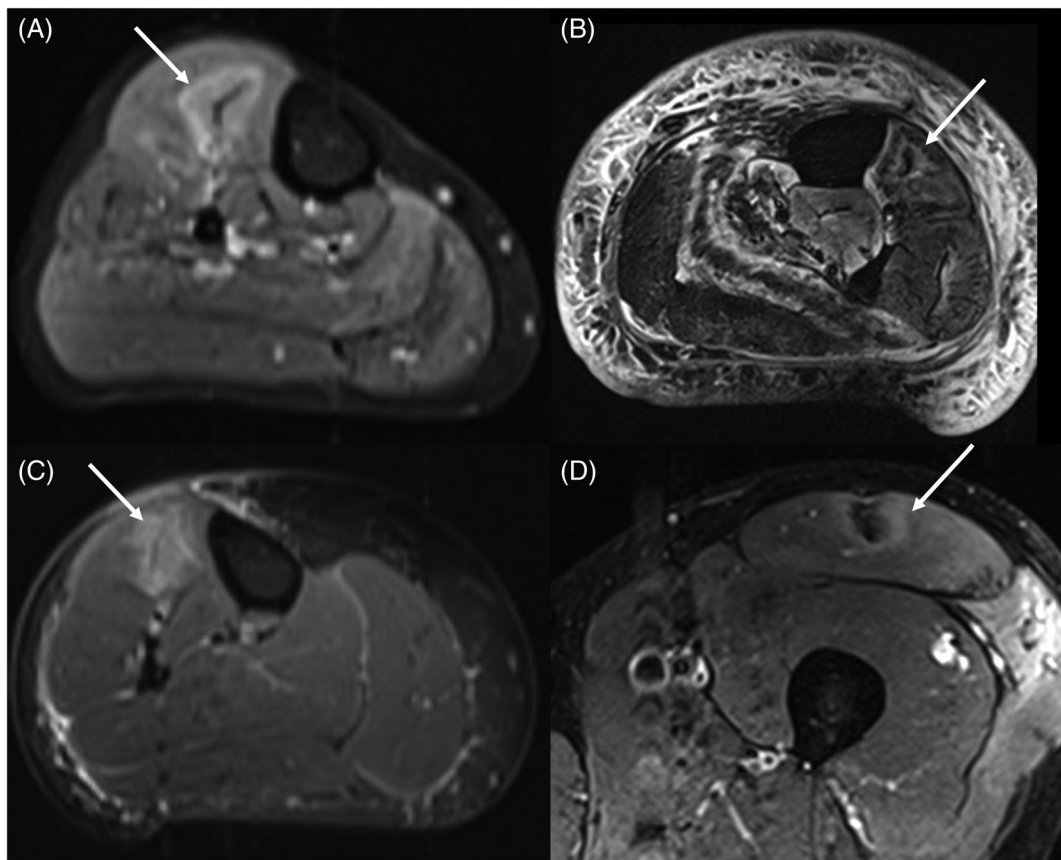


**FIGURE 5** Axial STIR MRI demonstrating peri-tendinous hyperintensity. (A) T2-STIR axial images of calf muscles demonstrating increased signal surrounding the tibialis anterior tendon (arrow). (B) T2-STIR axial images of thigh muscles demonstrating increased signal surrounding rectus femoris fascia/tendon (arrow).

weakness and a quarter required a gait aid or wheelchair. This is a significant burden of disease in a young patient cohort.

In seven patients (15.6%) we identified fat accumulation on MRI without fixed weakness. This highlights the potential advantage of MRI in detecting muscle changes before they can be clinically detected.

A small subset of our cohort had fixed weakness without episodic paralysis. These patients had a progressive myopathy phenotype and were most severely affected on MRI with correspondingly severe disability scores. Identifying these patients is important for prognostication and future planning for patients and family. Pelvic muscle involvement contributes to disability. This is illustrated by the clinically weak and disabled patients in our cohort with pelvic involvement but no lower leg involvement on MRI. Pelvic muscle imaging should be considered in routine clinical practice.

#### 4.2 | Role of MRI in diagnostics and as a biomarker

We identified preferential compartment involvement for *SCN4A* and *KCNJ2* variants, which is likely to be helpful in distinguishing a patient presenting with genetically undifferentiated periodic paralysis, or in those in whom variants of uncertain significance are found on genetic

testing. Clinically, it is important to differentiate and identify patients with ATS as they have a risk of serious cardiac arrhythmias and require cardiology review and screening.<sup>16,17</sup>

Peri-tendinous STIR hyperintensity seen in several of our patients may be a specific sign of a genetic periodic paralysis and may be helpful in undifferentiated cases. Further investigation into this finding may yield pathological insights. In particular, the temporal proximity of this peri-tendinous hyperintensity to an attack may be interesting to explore as well as comparison to changes seen in other channelopathies such as the central strip seen in myotonia congenita.<sup>18</sup> We did not see this central strip in any PP patients.

As described, we were able to detect muscle involvement on MRI in patients who had not yet developed fixed myopathy. One longitudinal review explored serial MRI in seven patients with Thr704Met *SCN4A* mutations.<sup>5</sup> A follow-up MRI at 30 mo demonstrated progressive myopathy.<sup>5</sup> Single cases have also been reported with improvement of MRI features with treatment.<sup>19</sup> In one patient with hypoPP, changes in muscle edema over time were demonstrated with resolution of edema and improved mobility after treatment.<sup>20</sup> Longitudinal studies are required to assess the response to treatment using muscle MRI. The ability to detect subclinical muscle change may also make MRI a useful biomarker in future clinical trials.

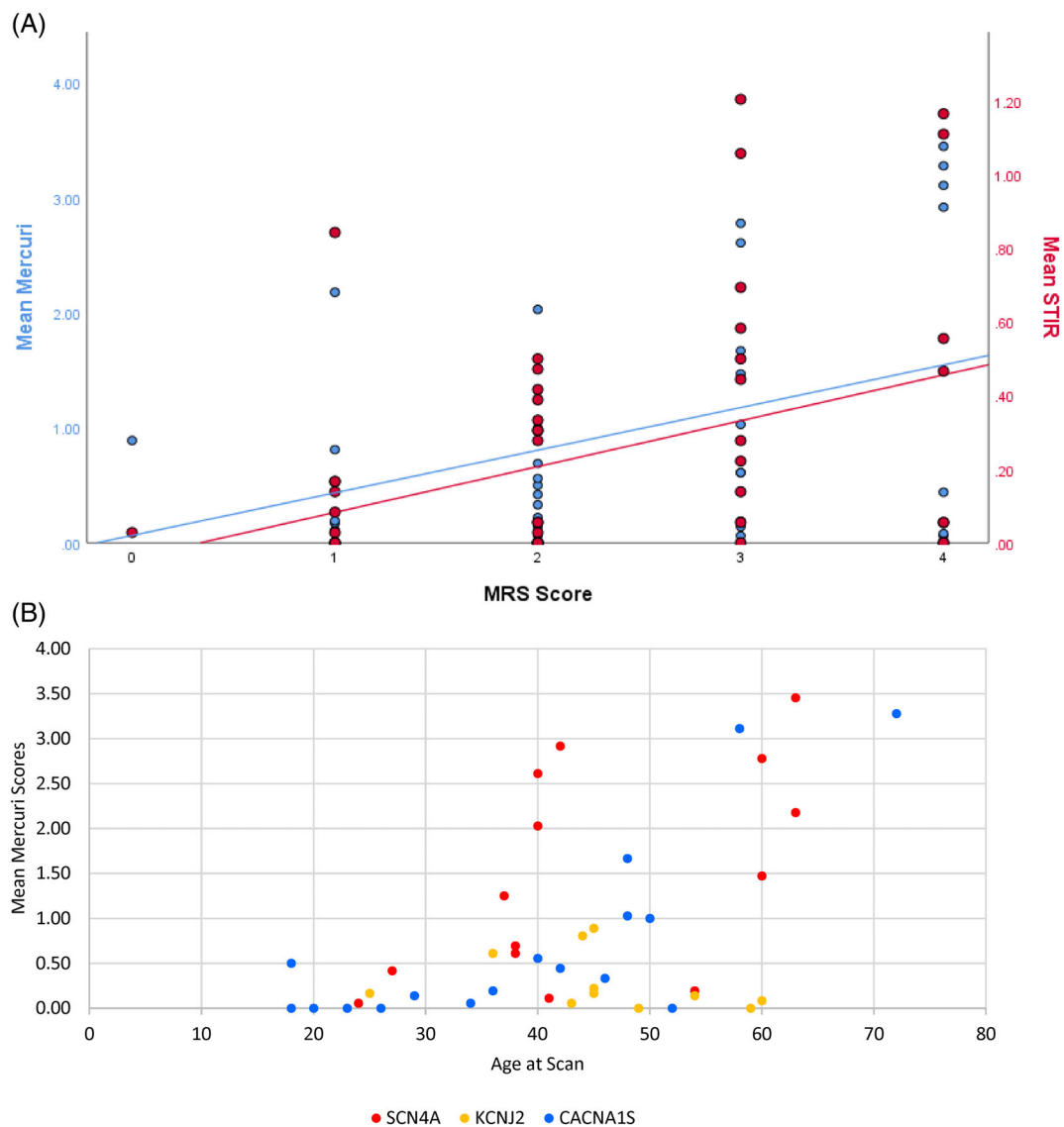


**FIGURE 6** (A) Scatter plot demonstrating correlation between MRS and mean Mercuri and STIR scores. R mean Mercuri scores = 0.36,  $P = .02$ ; R mean STIR score = 0.32,  $P = .03$ . (B) Scatter plot of age versus Mercuri scores.

While clinical trials have demonstrated improvement in attacks with treatment,<sup>21,22</sup> it remains unclear if medication treatment alters the natural history of the condition. The majority of our cohort were on treatment for periodic paralysis. Despite this, we found a significant burden of water deposition and fat accumulation on muscle MRI. Similar degrees of MRI involvement were seen in other publications with smaller percentages of untreated patients.<sup>6,7</sup> This may suggest that medications may provide only symptomatic treatment. Alternatively, more aggressive early treatment may be required to reduce intramuscular fat accumulation with increasing age. Further clinical trials are required to assess the impact of treatment. Additionally, larger studies are required to explore the correlation between disability, STIR hyperintensity and fat accumulation on MRI, which may be attractive outcome measures in future clinical trials.

The small number of healthy participants in this study is a limitation; however, it provides a sample of the acceptable degree of fat

accumulation and STIR in control patients, which supports previous reports in the literature.<sup>2</sup>

Overall, it is clear that the PP have marked morbidity, with two-thirds having clinical weakness and a quarter requiring a gait aid or wheelchair. Muscle MRI may assist in diagnosis by delineating patterns of muscle involvement, and it has potential use in future clinical trials. Our recommendations include the use of muscle MRI clinically in patients with undifferentiated episodic weakness (looking for patterns of involvement seen in *SCN4A* and *KCNJ2* as well as a distinctive pattern of peri-tendinous STIR hyperintensity), genetically confirmed patients without fixed myopathy to detect preclinical intramuscular fat accumulation, and consideration of pelvic imaging in patients with myopathy/disability and mild or no lower limb MRI involvement.

#### AUTHOR CONTRIBUTIONS

**Vinojini Vivekanandam:** Investigation; writing – original draft; methodology; validation; visualization; writing – review and editing; formal

analysis. **Karen Seutterlin:** Investigation; writing – review and editing. **Emma Matthews:** Writing – review and editing; supervision. **John Thornton:** Supervision; writing – review and editing. **Dipa Jayaseelan:** Writing – review and editing. **Sachit Shah:** Writing – review and editing; validation; investigation; formal analysis; supervision; resources. **Jasper Morrow M:** Investigation; writing – original draft; writing – review and editing; formal analysis; supervision. **Tarek Yousry:** Resources; writing – review and editing; supervision. **Michael Hanna FMedSci † 1 G:** Writing – review and editing; supervision; resources.

## ACKNOWLEDGMENTS

M.G.H. is supported by an MRC strategic award for International Centre for Genomic Medicine in Neuromuscular Diseases. V.V. is supported by the National Brain Appeal (Mission Possible, Dr. Hadi Manji). Our work is supported by the UCLH NIHR Biomedical Research Centre. We provide the only NHS England co-missioned national diagnostic service and references laboratory for children and adults muscle channelopathies led from University College London NHS Foundation Trust—for further details contact [m.hanna@ucl.ac.uk](mailto:m.hanna@ucl.ac.uk). The authors would like to sincerely thank all patients and families that participated in the study.

## CONFLICT OF INTEREST STATEMENT

None of the authors has any conflict of interest to disclose.

## DATA AVAILABILITY STATEMENT

The data that support the findings of this study are available from the corresponding author upon reasonable request.

## ETHICS STATEMENT

We confirm that we have read the Journal's position on issues involved in ethical publication and affirm that this report is consistent with those guidelines.

## ORCID

Vinojini Vivekanandam  <https://orcid.org/0000-0002-4944-0061>

## REFERENCES

- Vivekanandam V, Jaibaji R, Sud R, et al. Prevalence of genetically confirmed skeletal muscle Channelopathies in the era of next generation sequencing. *Neuromuscul Disord.* 2023;33:270-273. Published online: 2023. doi:10.1016/j.nmd.2023.01.007
- Morrow JM, Sinclair CDJ, Fischmann A, et al. MRI biomarker assessment of neuromuscular disease progression: a prospective observational cohort study. *Lancet Neurol.* 2016;15:65-77. Published online: 2016. doi:10.1016/S1474-4422(15)00242-2
- Bugiardini E, Morrow JM, Shah S, et al. The diagnostic value of MRI pattern recognition in distal myopathies. *Front Neurol.* 2018;9:1-11. Published online: 2018. doi:10.3389/fneur.2018.00456
- Kugathasan U, Evans MRB, Morrow JM, et al. Development of MRC Centre MRI calf muscle fat fraction protocol as a sensitive outcome measure in hereditary sensory neuropathy type 1. *J Neurol Neurosurg Psychiatry.* 2019;90:895-906. Published online: 2019. doi:10.1136/jnnp-2018-320198
- Jeong HN, Yi JS, Lee YH, et al. Lower-extremity magnetic resonance imaging in patients with hyperkalemic periodic paralysis carrying the SCN4A mutation T704M: 30-month follow-up of seven patients. *Neuromuscul Disord.* 2018;28:837-845. Published online: 2018. doi:10.1016/j.nmd.2018.06.008
- Maggi L, Brugnoli R, Canioni E, Maccagnano E, Bernasconi P, Morandi L. Imaging alterations in skeletal muscle channelopathies: a study in 15 patients. *Acta Myol: Myopathies Cardiomyopathies.* 2015;34:109-115. Published online: 2015.
- Holm-Yildiz S, Witting N, Dahlqvist J, et al. Permanent muscle weakness in hypokalemic periodic paralysis. *Neurology.* 2020;95:E342-E352. Published online: 2020. doi:10.1212/WNL.00000000000009828
- Jia BX, Yang Q, Li SY, et al. Muscle edema of the lower limb determined by mri in asian hypokalaemic periodic paralysis patients. *Neurol Res.* 2015;37:246-252. Published online: 2015. doi:10.1179/1743132814Y.00000000440
- Lee YH, Lee HS, Lee HE, et al. Whole-body muscle MRI in patients with hyperkalemic periodic paralysis carrying the SCN4A mutation T704M: evidence for chronic progressive myopathy with selective muscle involvement. *J Clin Neurol (Korea).* 2015;11:331-338. Published online: 2015. doi:10.3988/jcn.2015.11.4.331
- Bruno A, Akinwuntan AE, Lin C, et al. Simplified modified Rankin scale questionnaire. *Stroke.* 2011;42:2276-2279.
- Mercuri E, Talim B, Moghadasszadeh B, et al. Clinical and imaging findings in six cases of congenital muscular dystrophy with rigid spine syndrome linked to chromosome 1p (RSMD1). *Neuromusc Disord.* 2002;12:631-638. Published online: 2002. doi:10.1016/S0960-8966(02)00023-8
- Grevini S, Scarlato M, Maggi L, et al. Muscle MRI findings in facioscapulohumeral muscular dystrophy. *Eur Radiol.* 2016;26:693-705.
- Lim HK, Hong SH, Yoo HJ, et al. Visual MRI grading system to evaluate atrophy of the supraspinatus muscle. *Korean J Radiol.* 2014;15:501-507.
- Schober P, Schwarte LA. Correlation coefficients: appropriate use and interpretation. *Anesth Analg.* 2018;126:1763-1768. Published online: 2018. doi:10.1213/ANE.0000000000002864
- Cavel-Greant D, Lehmann-Horn F, Jurkat-Rott K. The impact of permanent muscle weakness on quality of life in periodic paralysis: a survey of 66 patients. *Acta Myol.* 2012;31:126-133. Published online: 2012.
- Maffè S, Paffoni P, Bergamasco L, et al. Therapeutic management of ventricular arrhythmias in Andersen-Tawil syndrome. *J Electrocardiol.* 2020;58:37-42. Published online: 2020. doi:10.1016/j.jelectrocard.2019.10.009
- Kukla P, Biernacka E, Baranchuk A, Jastrzebski M, Jagodzinska M. Electrocardiogram in Andersen-Tawil syndrome. New electrocardiographic criteria for diagnosis of Type-1 Andersen-Tawil syndrome. *Curr Cardiol Rev.* 2014;10:222-228. Published online: 2014. doi:10.2174/1573403x10666140514102528
- Morrow JM, Matthews E, Raja DL, et al. Muscle MRI reveals distinct abnormalities in genetically proven non-dystrophic myotonias. *Neuromuscul Disord.* 2013;23:637-646. Published online: 2013. doi:10.1016/j.nmd.2013.05.001
- Dejthevaporn C, Papsing C, Phakdeekitcharoen B, et al. Long-term effectiveness of acetazolamide on permanent weakness in hyperkalemic periodic paralysis. *Neuromuscul Disord.* 2013;23:445-449. Published online: 2013. doi:10.1016/j.nmd.2013.02.007
- Weber M-A, Jurkat-Rott K, Lerche H, Lehmann-Horn F. Strength and muscle structure preserved during long-term therapy in a patient with hypokalemic periodic paralysis (Cav1.1-R1239G). *J Neurol.* 2019. Published online: 2019;266:1623-1632. doi:10.1007/s00415-019-09302-3
- Statland JM, Fontaine B, Hanna MG, et al. Review of the diagnosis and treatment of periodic paralysis. *Muscle Nerve.* 2018;57:522-530. Published online: 2018. doi:10.1002/mus.26009

22. Tawil R, McDermott MP, Brown R, et al. Randomized trials of dichlorphenamide in the periodic paralyses. *Ann Neurol*. 2000;47:46-53. Published online: 2000. doi:[10.1002/1531-8249\(200001\)47:13.O.CO:2-H](https://doi.org/10.1002/1531-8249(200001)47:13.O.CO:2-H)

### SUPPORTING INFORMATION

Additional supporting information can be found online in the Supporting Information section at the end of this article.

**How to cite this article:** Vivekanandam V, Seutterlin K, Matthews E, et al. Muscle MRI in periodic paralysis shows myopathy is common and correlates with intramuscular fat accumulation. *Muscle & Nerve*. 2023;1-12. doi:[10.1002/mus.27947](https://doi.org/10.1002/mus.27947)